TÜBİTAK

Turkish Journal of Agriculture and Forestry

http://journals.tubitak.gov.tr/agriculture/

Research Article

Turk J Agric For
(2018) 42: 216-225

doi:10.3906/tar-1801-78

Application of data mining and adaptive neuro-fuzzy structure to predict color parameters of walnuts (*Juglans regia* L.)

Bünyamin DEMİR*

Department of Mechanical and Metal Technologies, Vocational School of Technical Sciences, Mersin University, Mersin, Turkey

Received: 17.01.2018 • **Accepted/Published Online:** 28.03.2018 • **Final Version:** 29.05.2018

Abstract: Quality is the primary factor designating consumer satisfaction and the market price of agricultural commodities. Color and general appearance are the basic quality indicators for agricultural products. Surface colors are assessed through colorimetric measurements including L*, a*, and b* color parameters. In the present study, L*, a*, and b* color parameters of Bilecik, Fernette, Fernor, Kaman-1, Maraş-12, Maraş-18, Sunland, Şen-2, Yalova-1, and Yalova-3 walnut cultivars (color parameters of 100 randomly selected walnuts from each cultivar) were measured with a chroma meter (CR-5 Konica Minolta). Based on L*, a*, and b* measurements, equations from which color index (*CI*), chroma (*C**), and hue (*h**) angle parameters could be calculated were developed with the Find Laws algorithm of PolyAnalyst. The color parameters obtained from these newly developed equations were used in training of adaptive neuro-fuzzy structure. Then color index (*CI*), chroma (*C**), and hue (*h**) angle parameters were predicted by adaptive neuro-fuzzy approach. Root mean square error values of the adaptive neuro-fuzzy-based approach were respectively identified as 0.02 for Bilecik, 0.01 for Fernette, 0.02 for Fernor, 0.01 for Kaman-1, 0.01 for Maraş-12, 0.01 for Maraş-18, 0.01 for Sunland, 0.01 for Şen-2, 0.01 for Yalova-1, and 0.01 for Yalova-3 walnuts. The obtained equations can be used as a viable alternative instead of equations that vary depending on whether a* and b* are negative or positive.

Key words: Neuro-fuzzy, estimation, walnut cultivars, color index, chroma, hue angle

1. Introduction

Walnut (*Juglans regia* L.) belongs to the family *Juglandaceae* (Şen, 2011). It ranks third in nut production worldwide after cashews and almonds (Amin et al., 2017). Walnuts are quite rich in oils, proteins, vitamins, fibers, minerals, and antioxidants; thus they are considered quite healthy nuts for human nutrition (Khir et al., 2014). Walnuts are used not only as an individual foodstuff, but also as an ingredient of several baked and processed foods (Eliseeva et al., 2017).

The physical properties of agricultural products have long attracted the attention of researchers (Bahrami et al., 2017). Previous researchers assessed the quality attributes of agricultural products such as shape, size, density, ripening level, moisture and oil content, firmness, flavor, and color of the products (Titova et al., 2015). The food industry uses various products in quite different sizes, colors, and shapes. Color can be used as a significant parameter in designing mechanical equipment to be used in sorting and grading processes of agricultural products (Mohsenin 1984; Pathare et al., 2013; Mahawar et al., 2017).

Quality standards for the nut and kernel of walnuts have already been established by the Turkish Standards Institute (TSE, 1990, 1991). Shell thickness, kernel size, kernel ratio, flavor, and kernel color are also indicated as significant quality attributes of walnuts (Warmund, 2008). The ones with symmetric or round shapes usually have higher market value than the others (Jun et al., 2017).

Color is considered a significant quality indicator for both raw and processed agricultural products since it is the first item perceived by consumers. It has a great potential to attract the attention and perceptions of buyers (Ellis and Kok, 2017; Goñi and Salvadori, 2017). For instance, for walnuts, light colors are usually preferred by consumers (Fuentealba et al., 2017).

The color of agricultural products is usually assessed through L*, a*, and b* values or CIELab color space (Goñi and Salvadori, 2017). CIELab color space is commonly used for comparing product colors (Rodríguez-Pulido et al., 2013). It is an international standard adopted by the Commission Internationale d'Eclairage (CIE) in 1976 for color measurements (León et al., 2006).

* Correspondence: bd@mersin.edu.tr

Color measurement instruments, usually colorimeters, are used to measure the color characteristics of agricultural products (Van Roy et al., 2017). Colorimeters also use CIELab color space and these instruments are used in quality assurance applications (Wickström et al., 2017). In CIELab color space, L* represents lightness and ranges between absolute black (L* = 0) and absolute white (L* = 100). The a* values are positive for reddish colors and negative for greenish colors. Similarly, b* takes positive values for yellowish colors and negative values for bluish colors. The a* and b* values are used to calculate C* (chroma) and h° (hue) angle values with the equations $C^* = (a^{*2} + b^{*2})^{1/2}$ and $h° = \tan^{-1} b^*/a^*$ (McGuire, 1992; Cáceres et al., 2016; Rodríguez-Pulido et al., 2017).

Several previous researchers used CIELab color space-based colorimeters to assess the color attributes of different fruit species (Sacks and Shaw, 1993; Heredia et al., 1998; Ayala-Silva et al., 2005; Christopoulos and Tsantili, 2011; Khir et al., 2014; Bujdoso et al., 2016; Cáceres et al., 2016; Amin et al., 2017; Cárdenas-Pérez et al., 2017; Kus et al., 2017; Udomkun et al., 2017), to assess the color attributes of different vegetable species (Kabelka et al., 2004; Colonna et al., 2016; Corona et al., 2016; De Oliveira Moura et al., 2016; Schoeninger et al., 2017; Zhang et al., 2017) and for various other food industry processes (Azabou et al., 2017; Guiné et al., 2017; Nascimento et al., 2017; Popa and Boran, 2017).

In recent years, artificial intelligence-based tools such as data mining and artificial neural networks have been applied for prediction of the physical properties of agricultural products (Demir et al., 2017; Eski et al., 2017; Kus et al., 2017; Gürbüz et al., 2018).

The present study was conducted to develop a new rule (equation) with Prediction and Find Laws algorithms of data mining to calculate color index (*CI*), chroma (C^*), and hue (h^*) angle parameters of 10 different walnut cultivars by using CIE-L*, a*, and b* values and to estimate the same color parameters calculated with this equation by using an adaptive neuro-fuzzy approach.

2. Materials and methods

The walnut cultivars Bilecik, Fernette, Fernor, Kaman-1, Maraş-12, Maraş-18, Sunland, Şen-2, Yalova-1, and Yalova-3 were used as the material of the present study. The walnuts were supplied by the Eğirdir Fruit Research Institute during the 2016 harvest season.

One hundred randomly selected walnuts of each cultivar were subjected to color measurements (Demir et al., 2017). Color measurements were performed over the outer surface of the walnut shells with a chroma meter (CR-5; Konica Minolta Bench-top, Japan). Measured CIE-L*, a*, and b* values were used to calculate color index (*CI*), hue angle (h^*), and chroma (C^*) values (McGuire, 1992):

$$CI = \frac{1000 \cdot a^*}{L^* \cdot b^*} \quad (1)$$

$$C^* = \sqrt{(a^*)^2 + (b^*)^2} \quad (2)$$

$$h^* = \tan^{-1}(b^* / a^*), \ (if \ a^* > 0 \ \ and \ b^* \geq 0) \quad (3)$$

$$h^* = 180 + \tan^{-1}(b^* / a^*), \ (if \ a^* < 0 \ \ and \ b^* \geq 0) \quad (4)$$

$$h^* = 180 + \tan^{-1}(b^* / a^*), \ (if \ a^* < 0 \ \ and \ b^* < 0) \quad (5)$$

$$h^* = 360 + \tan^{-1}(b^* / a^*), \ (if \ a^* > 0 \ \ and \ b^* < 0) \quad (6)$$

2.1. Prediction and Find Laws algorithms

Various methods have been developed for parameter estimations from real data. The Find Laws (FL) algorithm of PolyAnalyst is a common prediction engine used for parameter estimation. The algorithm yields complicated formulas expressing dependencies among real data. It employs symbolic knowledge acquisition technology and inquires operational relations in data. The rules can range from simple user-inputted equations to complex, high-degree rational polynomials generated by the FL algorithm. The ability of FL to automatically build a wide variety of mathematical constructions, including complex nonlinear algebraic expressions and functions, makes it a unique knowledge discovery tool. Resultant rules are mathematical expressions commonly used to generate a value based on a set of attributes (PolyAnalyst, 2007).

2.2. Predicted versus real graphs

The predicted versus real graph shows all the data points in the real dataset as well as model-predicted data points. Such presentation of the data points allows users to comprehend the accuracy and predictive power of the model. While the real data are placed on the x-axis, the predicted data are presented on the y-axis. When all the data points are quite close to the diagonal regression line, the predictive rule is considered perfect (PolyAnalyst, 2007).

2.3. Adaptive neuro-fuzzy interface system

The adaptive neuro-fuzzy interface system integrates a neural network with a fuzzy interface system (FIS). The FIS method is composed of 3 elements: a rule base, a database, and a reasoning mechanism. The adaptive neuro-fuzzy interface system uses two inputs (y_1 and y_2) and one output (v) to explain the fuzzy inference system. If the rule base contains a fuzzy set, if–then rules are applied as follows:

Rule 1: *If* y_1 *is* θ_1 *and* y_2 *is* β_1 *then* $v_1 = a_1 y_1 + b_1 y_2 + s_1$ (7)

Rule 2: *If* y_1 *is* θ_2 *and* y_2 *is* β_2 *then* $v_2 = a_2 y_1 + b_2 y_2 + s_2$, (8)

where θ_i and β_i are fuzzy membership sets, b_i is the number of membership equations, and s_i is the design parameter that is defined during the training process.

The adaptive neuro-fuzzy interface system consists of six layers as follows:

Layer 1: This is the input layer that determines actual data and desired data.

Layer 2: Each nodal in this layer is an adaptive nodal with a fuzzy membership equation. For two inputs, the nodal outputs are

$$L_i^1 = \alpha\theta_i(y), \qquad i=1,2 \tag{9}$$

$$L_i^1 = \alpha\beta_i(y), \qquad i=1,2, \tag{10}$$

where $\alpha\theta_i$ and $\alpha\beta_i$ are membership functions.

$$a\theta_i(y) = \frac{1}{1+\left[\left(\frac{y-p}{r_i}\right)^2\right]t_i}, \tag{11}$$

where $\{p_i, r_i, t_i\}$ is the coefficient group.

Layer 3: Each nodal in the third layer is a circle nodal called "Π", which multiples all signals and sends the product out.

$$w_i = \alpha\theta_i(y)\,\alpha\beta_i(y) \qquad (i=1,2..) \tag{12}$$

Layer 4: Each nodal in the fourth layer is a circle nodal called "Ɲ".

$$\overline{w}_i = \frac{w_i}{w_1 + w_2} \qquad (i=1,2..) \tag{13}$$

Layer 5: In this layer, each nodal i has the following function:

$$L_i^5 = \overline{w}_i f_i = \overline{w}_i(a_i y_1 + b_i y_2 + s_i) \tag{14}$$

Layer 6: The single nodal in the sixth layer is a circle nodal called "Σ".

$$L_i^6 = \sum \overline{w} f_i = \frac{\sum w_i f_i}{\sum w_i} \tag{15}$$

A schematic illustration of the adaptive neuro-fuzzy structure predictor is represented in Figure 1.

3. Results and discussion

The equations developed using L*, a*, and b* values of walnut cultivars as an alternative to formulations provided in the literature and cultivar-independent R^2 values of training and test data for *CI*, *C**, and *h** parameters estimated with these equations are provided in Table 1.

Randomly selected 70% of the data (700 items of data) were used for training and the remaining data (300 items of data) were used for testing. R^2 values for testing and training processes were respectively calculated as 1 and 0.99.

As seen from R^2 values, significant rules were obtained for predicting the color parameters of all types of walnut. This means the predicted values by the FL were almost equal to the target output.

The results in Figures 2–4 showed that adequate prediction was obtained with the predicted versus real graph of *CI*, *C**, and *h** by FL.

In Figures 2–4, the horizontal axis represents actual values of *CI*, *C**, and *h** parameters and the vertical axis represents estimated values of *CI*, *C**, and *h** parameters.

The results in Figures 5–7 showed that adequate prediction was obtained with the predicted and real versus counter of *CI*, *C**, and *h** by FL.

In Figures 5–7, record numbers of *CI*, *C**, and *h** parameters were provided on the horizontal axis and the actual and estimated values of *CI*, *C**, and *h** parameters were provided on the vertical axis.

The parameters calculated with the new equations were used to train the adaptive neuro-fuzzy structure.

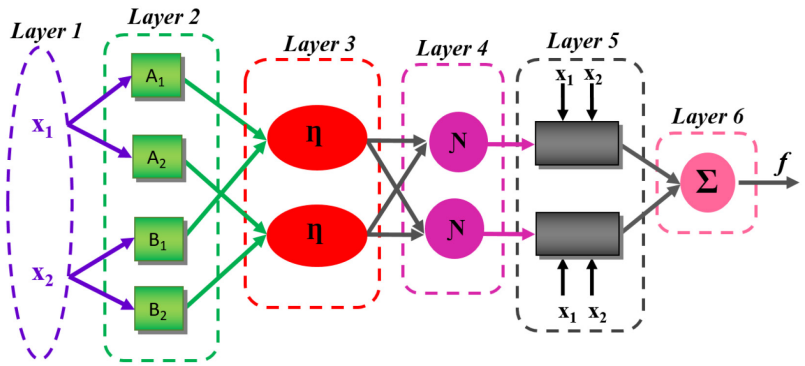

Figure 1. Schematic illustration of the adaptive neuro-fuzzy structure predictor.

Table 1. Prediction results for *CI*, *C**, and *h**.

Predicted parameter	Rule obtained	R^2 training value	R^2 test value
*CI**	$(-2466.09 *h*L+668383 *L-6.15865e^{+006} +23100.2 *h)/(h*L^2-1069.03 *L-107.365 *L^2)$	1	1
*C**	$-3.29937e^{+007} *a*b/(a-3.29937e^{+007})$	1	1
*h**	$(-2.91915e^{-007} *L*CI^4+304.96 *L*CI^3-0.079729 *L^2*CI^4-134795 *CI^2)/(L*CI^3-1.02014e^{-007} *L^3*CI^5-496.48 *CI^2)$	1	0.999

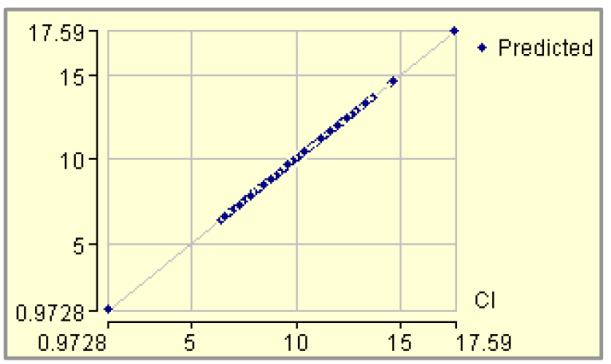

Figure 2. The predicted versus real graph of *CI* by FL.

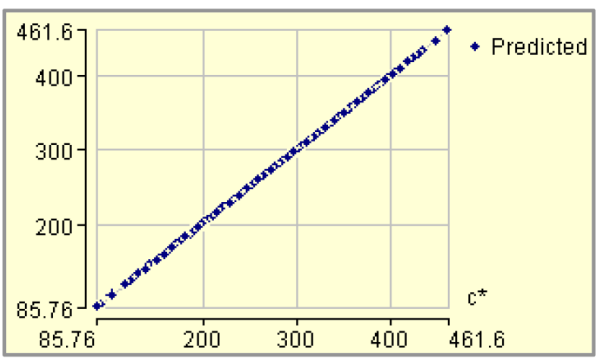

Figure 3. The predicted versus real graph of *C** by FL.

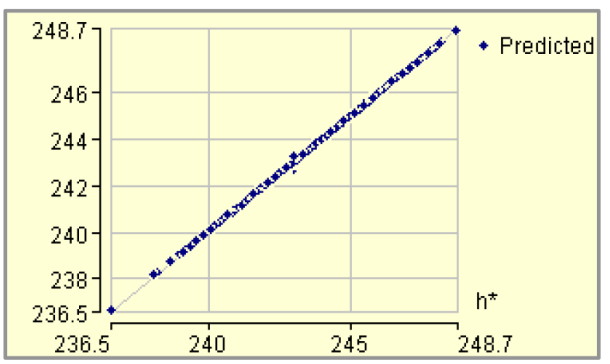

Figure 4. The predicted versus real graph of *h** by FL.

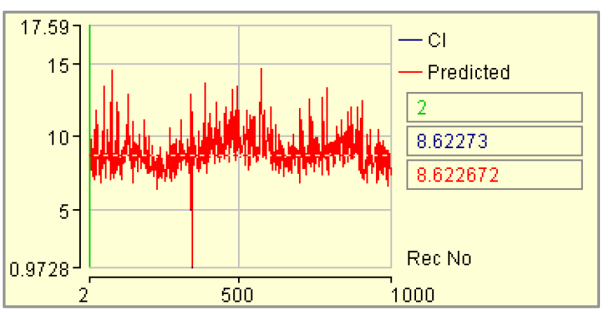

Figure 5. The predicted and real versus counter of *CI* by FL.

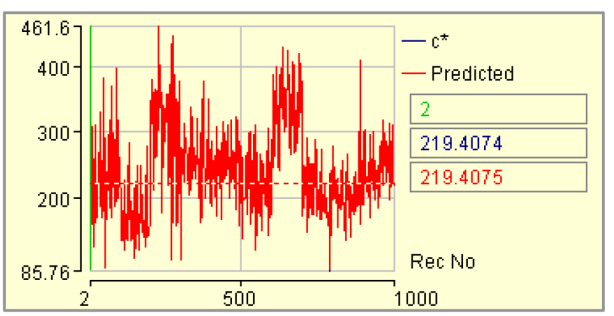

Figure 6. The predicted and real versus counter of *C** by FL.

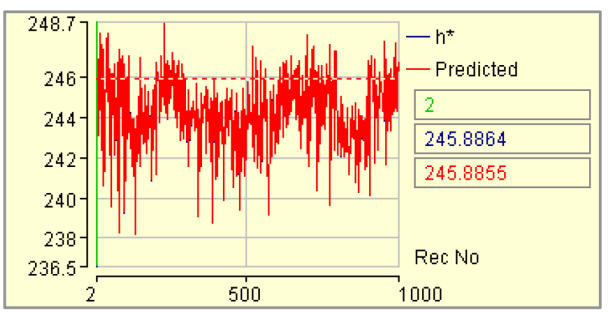

Figure 7. The predicted and real versus counter of *h** by FL.

Prediction results of the neuro-fuzzy structure for *CI*, *C**, and *h** parameters of each walnut cultivar are presented in graphs. In Figure 8, the dashed line shows the calculated data and the solid line shows predictions of the adaptive neuro-fuzzy structure. The predictions for the Yalova-1 cultivar with a root mean square error (RMSE) value of 0.01 were quite good (Table 2). Adaptive neuro-fuzzy predictions for the Bilecik and Fernor walnut cultivars are presented in Figures 9 and 10. Prediction results with an RMSE value of 0.02 were good. Figures 11 and 12 present predicted and calculated results for the Maraş-12 and Maraş-18 walnut cultivars. Prediction results for *CI*, *C**, and *h** parameters of the Kaman-1 and Fernette cultivars are presented in Figures 13 and 14. The results with an RMSE value of 0.01 were considered quite good. Prediction results for the Sunland and Yalova-3 walnut cultivars are presented in Figures 15 and 16 and the results for the Şen-2 cultivar are presented in Figure 17. Experimental and simulation results revealed that the adaptive neuro-fuzzy structure was able to predict *CI*, *C**, and *h** parameters with the least error by using L*, a*, and b* parameters. It is quite a tiresome and troublesome process to calculate color characteristics of walnut cultivars with the equations in the literature. However, color characteristics of a walnut cultivar can be predicted with an adaptive neuro-fuzzy structure trained for another walnut cultivar. Neural network-based structures can also be used to estimate physical, pomological, and color characteristics of several other agricultural products.

In a previous study, Demir et al. (2018a) used physical attributes and developed quite accurate rules to predict the width and depth of stalk cavity and eye basin of different apple varieties. In another study, Demir et al. (2018b) used

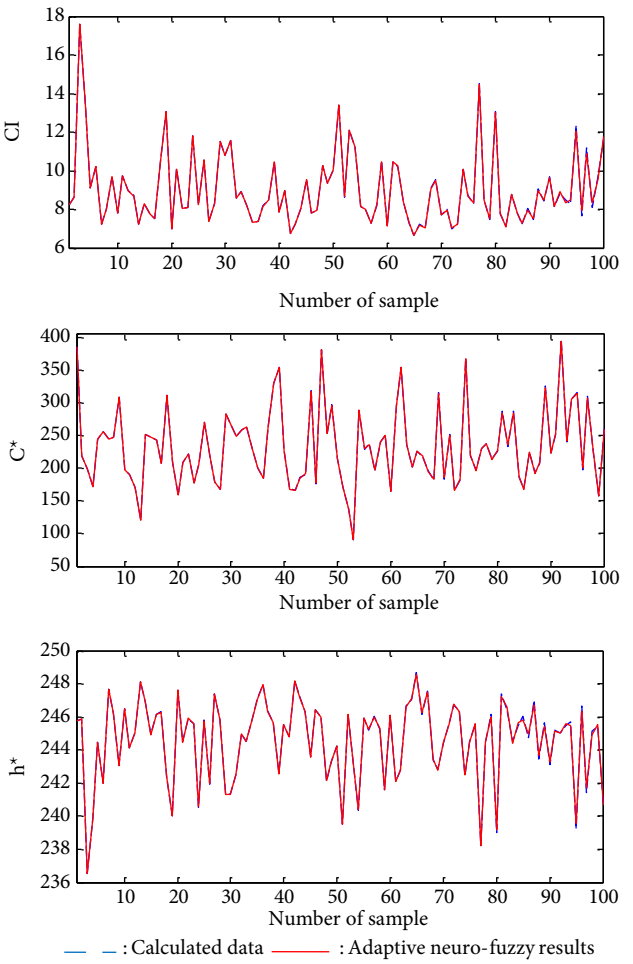

Figure 8. Adaptive neuro-fuzzy structure estimation results for Yalova-1.

Table 2. Neural network parameters of adaptive neuro-fuzzy approach.

NN type	η	α	N	RMSEs	
Adaptive neuro-fuzzy structure	0.1	0.6	4,000,000	Yalova-1	0.01
				Bilecik	0.02
				Fernor	0.02
				Maraş-12	0.01
				Maraş-18	0.01
				Kaman-1	0.01
				Fernette	0.01
				Sunland	0.01
				Yalova-3	0.01
				Şen-2	0.01

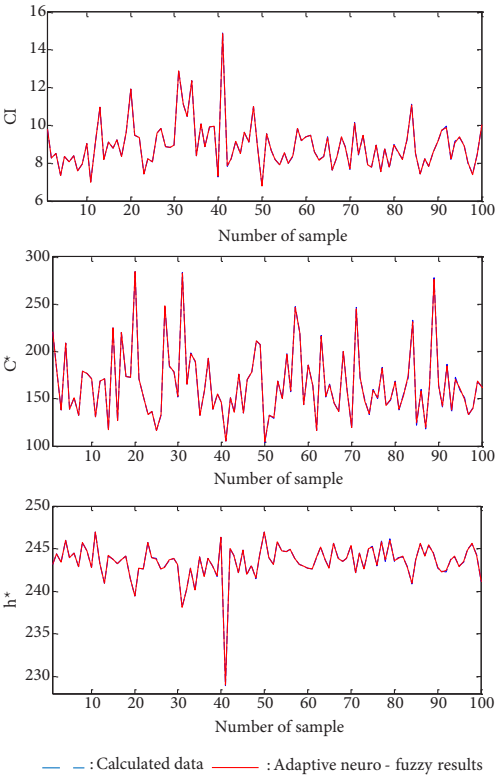

Figure 9. Adaptive neuro-fuzzy structure estimation results for Bilecik.

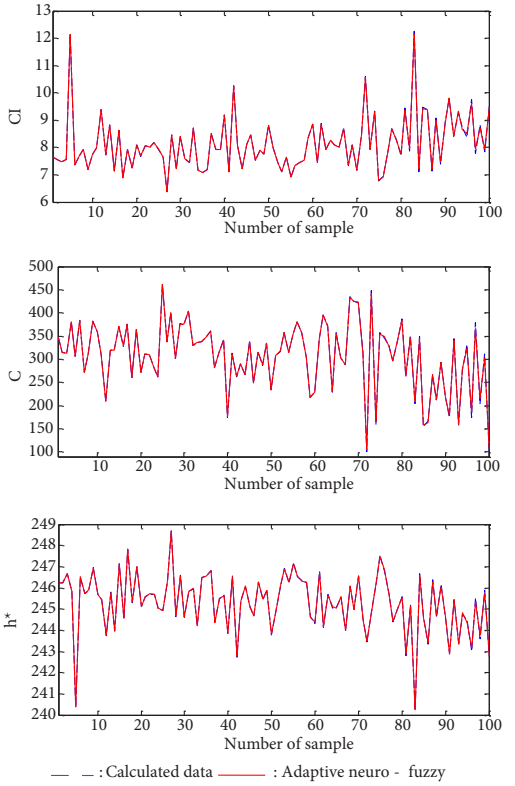

Figure 10. Adaptive neuro-fuzzy structure estimation results for Fernor.

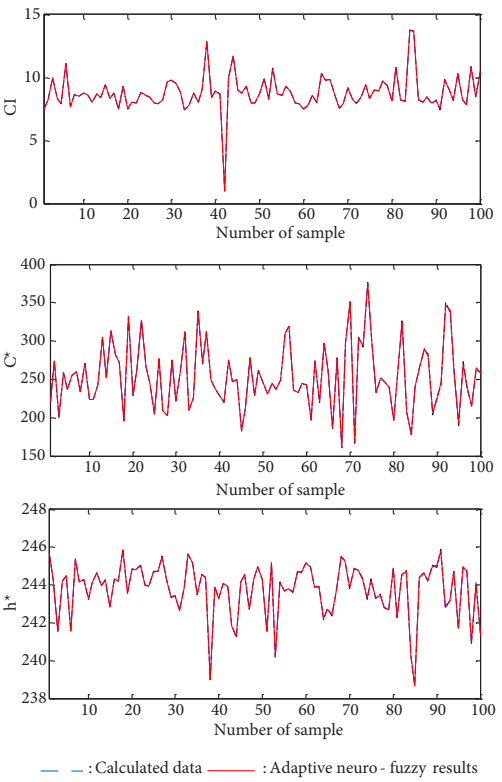

Figure 11. Adaptive neuro-fuzzy structure estimation results for Maraş-12.

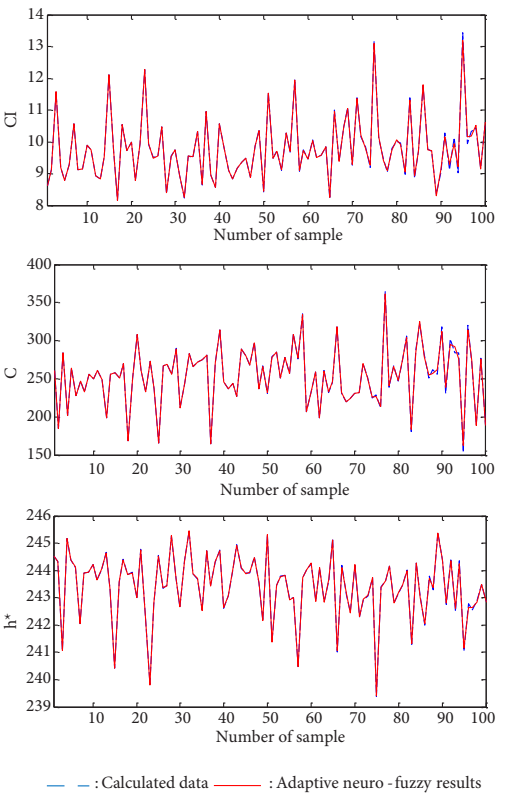

Figure 12. Adaptive neuro-fuzzy structure estimation results for Maraş-18.

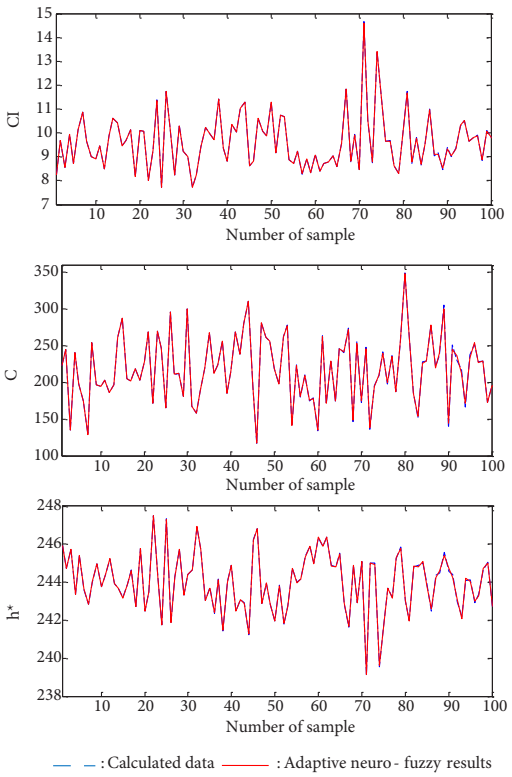

Figure 13. Adaptive neuro-fuzzy structure estimation results for Kaman-1.

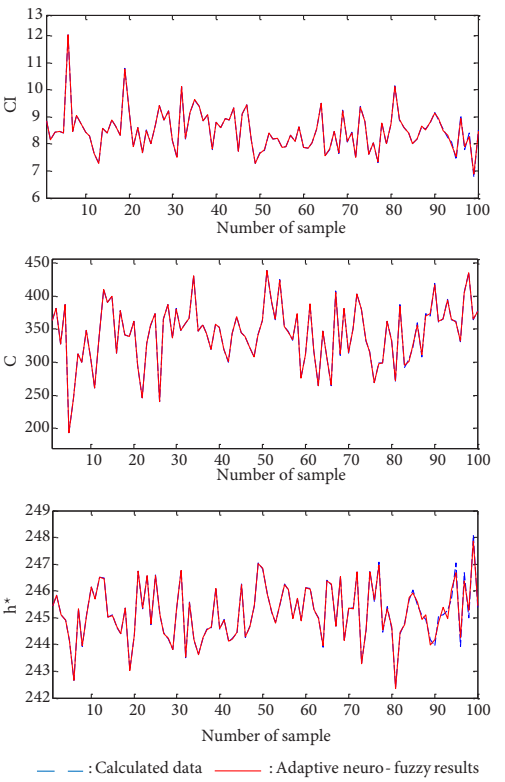

Figure 14. Adaptive neuro-fuzzy structure estimation results for Fernette.

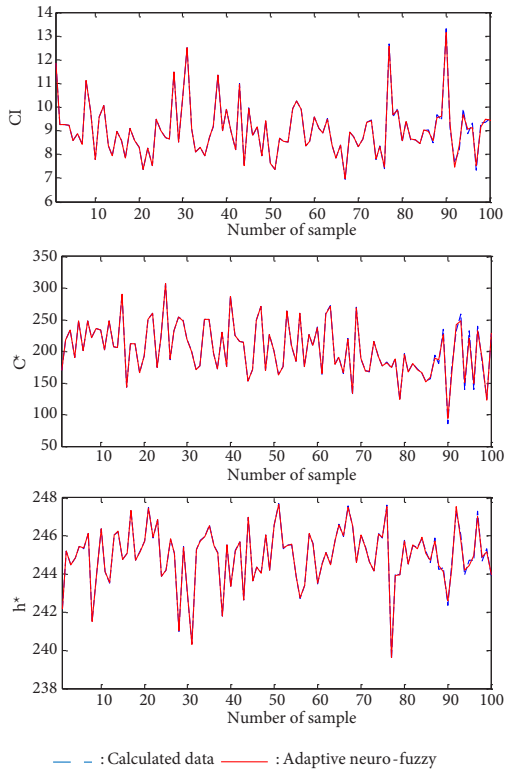

Figure 15. Adaptive neuro-fuzzy structure estimation results for Sunland.

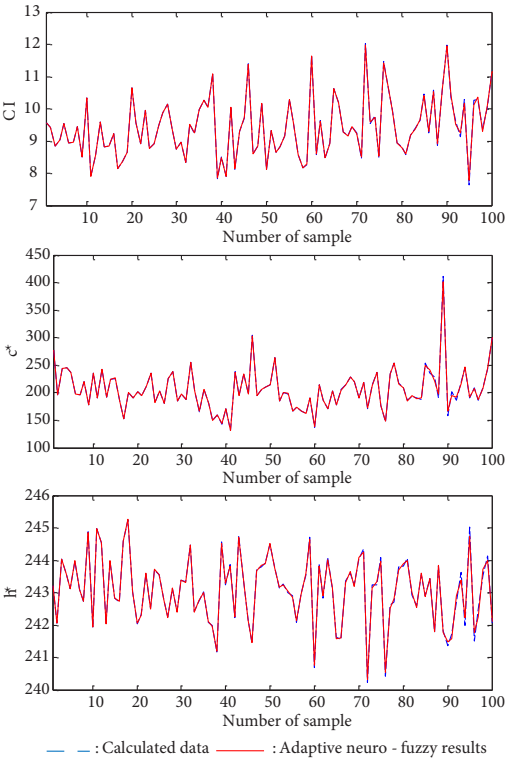

Figure 16. Adaptive neuro-fuzzy structure estimation results for Yalova-3.

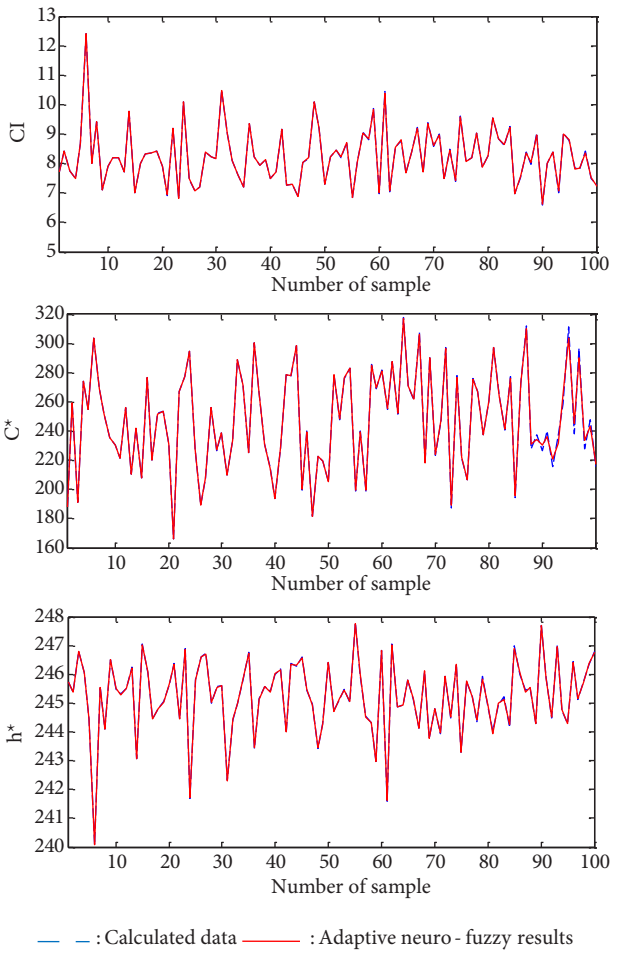

Figure 17. Adaptive neuro-fuzzy structure estimation results for Şen-2.

data mining approaches to predict color properties of fruits and developed rules with the FL algorithm of the data mining approach to estimate the color parameters (color index, hue angle, and chroma) of fruits. Gürbüz et al. (2018) estimated the weight of almond nuts from the physical attributes with data mining approaches and developed a highly accurate equation to calculate nut weights. Kus et al. (2017) predicted the hue angle, chroma, and color index of six apple varieties through artificial neural networks. According to the experimental and simulation results, the proposed ANFIS predictor had a superior performance in prediction of these color parameters. Demir et al. (2017) used two NN structures in the prediction of some physical parameters of pumpkin seeds. The RBNN had superior performance to predict different physical parameters of the pumpkin seeds.

Classifications are made in several agricultural products based on measured and calculated parameters. Color is a significant parameter for color standardization of agricultural products and for machine vision systems able to make color-dependent classifications.

Color-dependent manual grading of walnuts is a time-consuming and inconsistent process. Rapid and objective color measurements are required for classification and quality control of agricultural products like walnuts.

It was concluded that data mining could be used as an efficient tool to estimate the parameter values that are difficult to measure directly from the values of easily measured parameters. Therefore, the method can reliably be used in agricultural crops including vast amount of data. The present simulation results and error values revealed that the recommended adaptive neuro-fuzzy predictor was quite reliable in prediction of color index, chroma, and hue angle values of different walnut cultivars. The results also demonstrated that the adaptive neuro-fuzzy model successfully achieved quite high accuracy rates.

References

Amin F, Masoodi FA, Baba WN, Khan AA, Ganie BA (2017). Effect of different ripening stages on walnut kernel quality: antioxidant activities, lipid characterization and antibacterial properties. J Food Sci Tech 54: 3791-3801.

Ayala-Silva T, Schnell RJ, Meerow AW, Winterstein M, Cervantes C, Brown JS (2005). Determination of color and fruit traits of half-sib families of mango (*Mangifera indica* L.). In Proc Fla State Hort Soc 118: 253-257.

Azabou S, Taheur FB, Jridi M, Bouaziz M, Nasri M (2017). Discarded seeds from red pepper (*Capsicum annum*) processing industry as a sustainable source of high added-value compounds and edible oil. Environ Sci Pollut Res 24: 22196-22203.

Bahrami ME, Honarvar M, Ansari K (2017). Feasibility of using digital image processing and colorimetric measurements to estimate the physicochemical properties of raw cane sugars. Sugar Tech 19: 305-316.

Bujdoso G, Konya E, Berki M, Nagy-Gasztonyi M, Bartha-Szuegyi K, Marton B, Adányi N (2016). Fatty acid composition, oxidative stability, and antioxidant properties of some Hungarian and other Persian walnut cultivars. Turk J Agric For 40: 160-168.

Cáceres D, Díaz M, Shinya P, Infante R (2016). Assessment of peach internal flesh browning through colorimetric measures. Postharvest Biol Tec 111: 48-52.

Cárdenas-Pérez S, Méndez-Méndez JV, Chanona-Pérez JJ, Zdunek A, Güemes-Vera N, Calderón-Domínguez G, Rodríguez-González F (2017). Prediction of the nanomechanical properties of apple tissue during its ripening process from its firmness, color and microstructural parameters. Innov Food Sci Emerg 39: 79-87.

Christopoulos MV, Tsantili E (2011). Effects of temperature and packaging atmosphere on total antioxidants and colour of walnut (*Juglans regia* L.) kernels during storage. Sci Hortic 131: 49-57.

Colonna E, Rouphael Y, Barbieri G, De Pascale S (2016). Nutritional quality of ten leafy vegetables harvested at two light intensities. Food Chem 199: 702-710.

Corona O, Randazzo W, Miceli A, Guarcello R, Francesca N, Erten H, Settanni L (2016). Characterization of kefir-like beverages produced from vegetable juices. LWT-Food Sci Tech 66: 572-581.

De Oliveira Moura L, de Carvalho Lopes D, Neto AJS, Ferraz LDCL, de Almeida Carlos L, Martins LM (2016). Evaluation of techniques for automatic classification of lettuce based on spectral reflectance. Food Anal Methods 9: 1799-1806.

Demir B, Eski I, Kuş ZA, Ercisli S (2017). Prediction of physical parameters of pumpkin seeds using neural network. Not Bot Horti Agrobot Cluj Napoca 45: 22-27.

Demir B, Gurbuz F, Eski I, Kus ZA, Yilmaz KU, Ercisli S (2018a). Possible use of data mining for analysis and prediction of apple physical properties. Erwerbs-Obstbau 60: 1-7.

Demir B, Gurbuz F, Eski İ, Kuş ZA (2018b). Data mining approach for prediction of fruit color properties. Atatürk University Journal of the Agricultural Faculty 49: 37-43.

Eliseeva L, Yurina O, Hovhannisyan N (2017). Nuts as raw material for confectionary industry. Ann Agrar Sci 15: 71-74.

Ellis LP, Kok C (2017). Colour changes in Blanc de Noir wines during ageing at different temperatures and its colour preference limits. S Afr J Enol Vitic: 8: 16-22.

Eski İ, Demir B, Gürbüz F, Kuş ZA, Yilmaz KU, Uzun M, Ercişli S (2017). Design of neural network predictor for the physical properties of almond nuts. Erwerbs-Obstbau doi:10.1007/s10341-017-0349-3

Fuentealba C, Hernández I, Saa S, Toledo L, Burdiles P, Chirinos R, Pedreschi R (2017). Colour and in vitro quality attributes of walnuts from different growing conditions correlate with key precursors of primary and secondary metabolism. Food Chem 232: 664-672.

Goñi SM, Salvadori VO (2017). Color measurement: comparison of colorimeter vs. computer vision system. J Food Meas Charact 11: 538-547.

Guiné R, Leitão S, Gonçalves F, Correia P (2017). Evaluation of colour in a newly developed food product: fresh cheese with red fruits. J Sci Eng Res 4: 108-115.

Gurbuz F, Demir B, Eski I, Kus ZA, Yilmaz KU, İlikçioğlu E, Ercisli S (2018). Estimation of the weights of almond nuts based on physical properties through data mining. Not Bot Horti Agrobot Cluj Napoca doi: 10.15835/nbha46210631.

Heredia FJ, Francia-Aricha EM, Rivas-Gonzalo JC, Vicario IM, Santos-Buelga C (1998). Chromatic characterization of anthocyanins from red grapes—I. pH effect. Food Chem 63: 491-498.

Jun LU, Han XZ, Wang KJ (2017). Classification of Collection Walnut Based on GLCM and SVM. 2nd International Conference on Test, Measurement and Computational Method (TMCM 2017), pp: 276-281.

Kabelka E, Yang W, Francis DM (2004). Improved tomato fruit color within an inbred backcross line derived from *Lycopersicon esculentum* and *L. hirsutum* involves the interaction of loci. J Am Soc Hortic Sci 129: 250-257.

Khir R, Atungulu GG, Pan Z, Thompson JF, Zheng X (2014). Moisture-dependent color characteristics of walnuts. Int J Food Prop 17: 877-890.

Kus ZA, Demir B, Eski I, Gurbuz F, Ercisli S (2017). Estimation of the colour properties of apples varieties using neural network. Erwerbs-Obstbau 59: 291-299.

León K, Mery D, Pedreschi F, León J (2006). Color measurement in L*a*b*, units from RGB digital images. Food Res Int 39: 1084-1091.

Mahawar MK, Jalgaonkar K, Kumar M, Meena VS, Bhushan B (2017). Determination of some physical properties of date palm fruits (cv. Khadrawy and medjool). Acta Agroph 24: 217-223.

McGuire RG (1992). Reporting of objective color measurements. HortScience 27: 1254-1255.

Mohsenin NN (1984). Electromagnetic Radiation Properties of Foods and Agricultural Products. Gordon and Breach Science Publishers: New York, NY, USA, 1984.

Nascimento EDA, Melo EDA, Lima VLAGD (2017). Ice cream with functional potential added grape agro-industrial waste. J Culinary Sci Tech 2017: 1-21.

Pathare PB, Opara UL, Al-Said FAJ (2013). Colour measurement and analysis in fresh and processed foods: a review. Food Bioprocess Tech 6: 36-60.

PolyAnalyst (2007). User Manual of PolyAnalyst 6.5, April 2007.

Popa S, Boran S (2017). CIELAB and thermal properties of sesame food oil under antocyanin and UV influence. Rev Chim 68: 1401-1405.

Rodríguez-Pulido FJ, Gordillo B, González-Miret ML, Heredia FJ (2013). Analysis of food appearance properties by computer vision applying ellipsoids to colour data. Comput Electron Agr 99: 108-115.

Rodríguez-Pulido FJ, Gil-Vicente M, Gordillo B, Heredia FJ, González-Miret ML (2017). Measurement of ripening of raspberries (*Rubus idaeus* L) by near infrared and colorimetric imaging techniques. J Food Sci Tech 54: 2797-2803.

Sacks EJ, Shaw DV (1993). Color change in fresh strawberry fruit of seven genotypes stored at 0C. HortScience 28: 209-210.

Schoeninger V, Coelho SRM, Bassinello PZ (2017). Industrial processing of canned beans. Cienc Rural 47: 1-9.

Şen SM (2011). Ceviz Yetiştiriciliği, Besin Değeri, Folklorü. 4th edition. Ankara, Turkey: ÜÇM Yayıncılık.

Titova TP, Nachev VG, Damyanov CI (2015). Food quality evaluation according to their color characteristics. FU Aut Cont Rob 14: 1-10.

TSE (1990). Unshelled walnuts. Turkish Standard Institute (T.S.E.), TS 1275, Ankara, Turkey.

TSE (1991). Walnut kernels. Turkish Standard Institute (T.S.E.), TS 1276, Ankara, Turkey.

Udomkun P, Nagle M, Argyropoulos D, Wiredu AN, Mahayothee B, Müller J (2017). Computer vision coupled with laser backscattering for non-destructive colour evaluation of papaya during drying. J Food Meas Charact 11: 2142-2150.

Van Roy J, Keresztes JC, Wouters N, De Ketelaere B, Saeys W (2017). Measuring colour of vine tomatoes using hyperspectral imaging. Postharvest Biol Tec 129: 79-89.

Warmund MR (2008). Kernel color of three black walnut cultivars after delayed hulling at five successive harvest dates. HortScience 43: 2256-2258.

Wickström H, Nyman JO, Indola M, Sundelin H, Kronberg L, Preis M, Sandler N (2017). Colorimetry as quality control tool for individual inkjet-printed pediatric formulations. AAPS Pharm Sci Tech 18: 293-302.

Zhang S, Zhu Y, You Z, Wu X (2017). Fusion of superpixel, expectation maximization and PHOG for recognizing cucumber diseases. Comput Electron Agr 140: 338-347.